Automated Discovery of Denial-of-Service Vulnerabilities in Connected Vehicle Protocols

Shengtuo Hu, *University of Michigan;* Qi Alfred Chen, *UC Irvine;* Jiachen Sun, Yiheng Feng, Z. Morley Mao, and Henry X. Liu, *University of Michigan*

https://www.usenix.org/conference/usenixsecurity21/presentation/hu-shengtuo

This paper is included in the Proceedings of the 30th USENIX Security Symposium.

August 11–13, 2021

978-1-939133-24-3

Open access to the Proceedings of the 30th USENIX Security Symposium is sponsored by USENIX.

Automated Discovery of Denial-of-Service Vulnerabilities in Connected Vehicle Protocols

Shengtuo Hu
University of Michigan

Qi Alfred Chen
UC Irvine

Jiachen Sun
University of Michigan

Yiheng Feng
University of Michigan

Z. Morley Mao
University of Michigan

Henry X. Liu
University of Michigan

Abstract

With the development of the emerging Connected Vehicle (CV) technology, vehicles can wirelessly communicate with traffic infrastructure and other vehicles to exchange safety and mobility information in real time. However, the integrated communication capability inevitably increases the attack surface of vehicles, which can be exploited to cause safety hazard on the road. Thus, it is highly desirable to systematically understand design-level flaws in the current CV network stack as well as in CV applications, and the corresponding security/safety consequences so that these flaws can be proactively discovered and addressed before large-scale deployment.

In this paper, we design *CVAnalyzer*, a system for discovering design-level flaws for *availability* violations of the CV network stack, as well as quantifying the corresponding security/safety consequences. To achieve this, *CVAnalyzer* combines the attack discovery capability of a general model checker and the quantitative threat assessment capability of a probabilistic model checker. Using *CVAnalyzer*, we successfully uncovered 4 *new* DoS (Denial-of-Service) vulnerabilities of the *latest* CV network protocols and 14 new DoS vulnerabilities of two CV platoon management protocols. Our quantification results show that these attacks can have as high as 99% success rates, and in the worst case can at least double the delay in packet processing, violating the latency requirement in CV communication. We implemented and validated all attacks in a real-world testbed, and also analyzed the fundamental causes to propose potential solutions. We have reported our findings in the CV network protocols to the IEEE 1609 Working Group, and the group has acknowledged the discovered vulnerabilities and plans to adopt our solutions.

1 Introduction

With the emerging Connected Vehicle (CV) technology [64], Vehicle-to-Vehicle (V2V) and Vehicle-to-Infrastructure (V2I) wireless communication enables vehicles to exchange important safety and mobility information with other entities in real time. In September 2016, the U.S. Department of Transportation (USDOT) launched the CV Pilot Program in three sites, New York City, Wyoming, and Tampa, to spur early CV technology deployment and test CV safety applications in the real world. As of Fall 2018, the program has entered the third phase, which requires at least 18-month period for long-term operation and key performance measurements [66].

While CV technology can greatly benefit transportation mobility and safety, such dramatically increased connectivity inevitably increases the attack surface of both vehicles and the transportation infrastructure. For example, if the CV communication protocol stack is not sufficiently secure, attackers can directly cause safety hazard to human drivers on the road [1, 13, 45]. Thus, it is imperative to understand the potential security vulnerabilities in the CV network stack as early as possible so that they can be proactively addressed before large-scale deployment. To achieve this, it is necessary to start with a systematic study of potential design-level security flaws in the CV network stack, since both the discovery and defense solutions of such flaws can most generally affect the security of their corresponding implementation instances.

Existing work on the analysis of Vehicular Ad-Hoc Network (VANET) or CV security [1, 4, 10, 28, 29, 44, 55, 55, 73] generally suffer from three limitations:

(L1): they lack systematic approaches and rely on manual inspection to identify potential threats [1, 44, 55, 73], which is both insufficient and inefficient. It is also hard to automate the risk assessment of identified threats in these works. For example, Laurendeau et al. [44] use ETSI's threat analysis methodology [24], which relies on human to qualitatively rank the risks of the threats. Similarly, Petit et al. [55] manually characterized threats in the automated vehicle (e.g., the cooperative automated vehicle with V2X communication), only annotated the qualitative risk.

(L2): The threats to the availability of the higher-layer protocols (i.e., IEEE 1609 protocols [32, 34] and CV applications), which can prevent legitimate protocol participants from accessing critical services in the network, are largely under explored [4, 12, 28, 54, 65]. Although USDOT and the protocol designers have already employed security mechanisms to protect the integrity and confidentiality of CV network com-

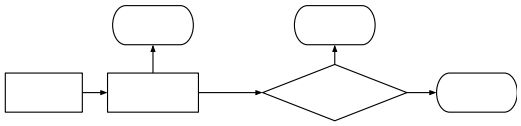

Figure 1: Verify-on-Demand [4, 41]: a connected vehicle will only verify the signatures of incoming packets, if packets result in a safety threat level above the threshold.

munication [4, 65], the protocol stack may still suffer from availability issues. For instance, as shown in Figure 1, if an incoming packet that may result in a safety threat cannot pass the verification, it will be discarded without triggering any warnings, and the application will not be able to process any incoming packets. To the best of our knowledge, only one prior work inspected the threats to availability [73], but it suffers from the third limitation below.

(L3): Previous works mostly target prior generations of the protocols, ignoring the analysis of CV applications, or are conducted before the standardization of IEEE 1609 protocol family, and hence some discovered vulnerabilities do not exist in the latest CV network stack design [4, 10, 29, 44, 55, 73]. For instance, the latest version of IEEE 1609.3[1] has integrated WAVE Service Advertisement (WSA) security considerations [73], in which Whyte et al. identify threats to availability of WSA in IEEE 1606.3-2010 [31] due to misconfigurations or malicious WSA access parameters.

In this paper, we perform the first rigorous security analysis to automate the discovery of availability or DoS (Denial of Service) vulnerabilities, in (1) the latest version of the IEEE 1609 protocol family and (2) Cooperative Adaptive Cruise Control (CACC) applications. To address L1 (i.e., manual analysis), we formulate the analysis as a model-checking problem and design a novel system, *CVAnalyzer*, that leverages (1) a general model checker (MC) [75] and (2) a probabilistic model checker (PMC) [42] to automate *both* the attack discovery and the attack assessment. Either model checker alone cannot achieve our analysis goal [8]. MC [16, 21, 27, 75] is useful for the attack discovery [9, 22, 26, 30, 48, 50]; while, for tractability reasons, PMC (e.g., PRISM [42]) has limited support in finding vulnerabilities and mainly focuses on quantitative property verification. Therefore, we utilize MC and PMC to verify availability-related properties and quantitative properties respectively.

To address L2 (i.e., no availability threat analysis), we define security properties to cover both availability-related properties (e.g., "all CV devices should eventually learn unknown certificates") and quantitative properties (e.g., "what is the expected time delay of processing next packet?"). By verifying these properties, we not only identify potential vulnerabilities but also understand the corresponding security consequences.

To address L3, we inspect the *latest* specifications [67] of the CV network protocols and one complicated CV application (i.e., CACC). For the former, we focus on *newly* added *CV-specific* features (e.g., P2PCD); for the latter, we pick two platoon management protcols (PMPs) (VENTOS [5, 69] and PLEXE [56, 60]), which are widely used by researchers, practitioners, and developers. We choose to study PMP because (1) high importance, since it can directly control vehicles and thus impact safety [1, 23], and (2) high demand for systematic verification, since it involves distributed collaboration among multiple vehicles and thus highly difficult to effectively analyze using only manual efforts. We abstract the CV protocols as multiple finite state machines (FSMs). In the abstract model, each FSM represents a protocol participant, and all participants communicate with each other through adversary-controlled public communication channels. Notably, such abstract model ignores the low-level implementation details, which is suitable for finding design flaws.

By design, *CVAnalyzer* does not trigger any false positives, aiming to guarantee *soundness*. That is, if we report a property violation, it is indeed a violation; we cannot, however, detect all violations. Like existing works on model checking security protocols [26, 30, 48], our analysis is parameterized by the number of protocol participants. Given a specific number of protocol participants and a set of properties, model checking guarantees to exhaustively enumerate all reachable states. Therefore, a model checker should also have *completeness*, i.e., if the model checker does not report any property violations, then the model is proved to be correct. However, due to the undecidability of parameterized system verification problem [6], achieving both soundness and completeness is impossible, and we cannot enumerate all possible number of protocol participants. In this case, we follow the conventional method of aiming for soundness instead of completeness.

In model checking, the model size (i.e., the total number of reachable states) grows exponentially with the number of state variables and the number of protocol participants. To alleviate the state explosion [18] problem in applying model checking to complex network protocols, we propose an *abstraction* approach (§ 4), which reduces unnecessary state variables and merges a large data domain into a small equivalent data domain. We ensure that our state reduction approach does not introduce wrong property violations (i.e., false positives).

Overall, our contributions are summarized as follows:

- We perform the *first* rigorous security analysis to find DoS attacks in the *latest* version of IEEE 1609 protocol family and two PMPs via the model checking technique. To achieve this goal, our analysis methodology design aims at providing soundness without triggering any false positives. To alleviate the state explosion problem, we propose a novel *abstraction* approach, which does not generate any false positives and can also achieve complete model coverage.
- Using *CVAnalyzer*, we are able to discover 4 *new* DoS vulnerabilities in P2PCD, which can block the certificate learning process and can further prevent the application

[1] In the following text, without specific notations, "IEEE 1609.*" represents the latest version (e.g., "IEEE 1609.2" and "IEEE 1609.3" stands for "IEEE 1609.2-2016" and "IEEE 1609.3-2016" respectively).

layer from processing incoming packets, and 15 vulnerabilities (14 of 15 are new) in PMPs, which can block the communication among platoon members. Our quantification results show that their exploits can have as high as 99% success rates, and can double the delay in packet processing, which violates the latency requirement of CV communication.

- For these newly-discovered vulnerabilities, we have constructed practical exploits and validated them in a real-world testbed. We have also reported to and received confirmations for P2PCD attacks from IEEE 1609 Working Group [35]. Besides, our case studies demonstrate that P2PCD attacks can lead to traffic accidents, and PMP attacks can affect the speed stability of the victim vehicle. These results thus concretely demonstrate the effectiveness of *CVAnalyzer*.
- For the identified vulnerabilities, we discuss the fundamental reasons and propose effective mitigation solutions, including avoiding using truncated hash value (e.g., 3-byte hash value), mandating verification for P2PCD learning responses, and requiring P2PCD learning requests to be broadcast (§7). After our discussion with the IEEE 1609 Working Group [35], mitigation solutions against P2PCD attacks are planned to be integrated into the next version of IEEE 1609.2.

2 Technical Background

In this section, we introduce the necessary technical background about the CV network stack and the platoon management protocols (PMPs).

2.1 CV Technology & Network Stack

CV network provides connectivity in support of mobile and stationary CV applications, which offers users greater situational awareness of events, potential threats, and imminent hazards, with the goal of enhancing the safety, mobility, and convenience of everyday transportation [36]. In the CV network, there are two basic types of devices: (1) On-Board Unit (OBU) in a roaming vehicle and (2) stationary Road-Side Unit (RSU) along the road. Usually, the communication pattern of the CV network is individual messages that are broadcast without response [34].

IEEE 802.11p [37] and its extension IEEE 1609.4 [33] together define the basis of the CV network stack, in which IEEE 802.11p disables the authentication, association, and data confidentiality services at the MAC layer to minimize the message latency. Above them, IEEE 1609.3 [34] defines the WAVE Short Message Protocol (WSMP), which is optimized to minimize communication overhead. The Basic Safety Message (BSM, a.k.a., the beacon message) defined in SAE J2735 is used by a variety of applications, such as Forward Collision Warning (FCW), Cooperative Adaptive Cruise Control (CACC), to exchange safety data regarding vehicle state (e.g., location and speed). The transmission rate of BSM is typically set to 10 times per second [2, 3, 25].

Due to the safety-critical nature of CV applications, IEEE 1609.2 [32] specifies security mechanisms to provide confidentiality, authenticity, integrity, and non-repudiation. It introduces digital certificates to enable digital signature (ECDSA), with the support of a Public-Key Infrastructure (PKI) system called Security Credential Management System (SCMS) [12]. Also, SCMS supports the misbehavior detection and certificate revocation to prevent malicious vehicles from communicating with others, while the development of the misbehavior detection algorithms is still ongoing.

In particular, IEEE 1609.2 specifies a unique feature called Peer-to-Peer Certificate Distribution (P2PCD) that helps a CV device to learn unknown certificates. When a device receives a signed secured protocol data unit (SPDU), it will construct a certificate chain for the signing certificate within the SPDU. The certificate chain links the signing certificate to a known *trust anchor*, which usually refers to the root certificates shared by all CV devices, so the incoming SPDU can be trusted by the receiver. However, the CV device may be unable to construct such a certificate chain due to not recognizing the issuer of the signing certificate. In this case, the received SPDU is referred to as a trigger SPDU, and the CV device will attach P2PCD learning request field in the next outgoing SPDU to request peer devices to provide the necessary certificates to complete the chain. P2PCD learning responses, which contains requested certificates, will be sent back through WSMP by peer devices. Note that, a P2PCD learning response is sent as a protocol data unit (PDU) rather than an SPDU. That is, the P2PCD learning response itself does not carry the digital signature. The current IEEE 1609.2 does not mention the verification for the payload of the learning response (cf. IEEE 1609.2-2016, Clause 8.2.4.1 c)). Besides, the P2PCD example in IEEE 1609.2 (cf. 1609.2-2016 Clause D.4.3.6) only considers `VerifyCertificate` primitive as an optional step before `AddCertificate` primitive.

2.2 Platoon Management Protocol (PMP)

CVs form a platoon with minimal following distances to improve traffic density and fuel economy. The PMP is an essential component for platoon applications to control platoon maneuvers. Typically, vehicles in a platoon exchange speed, location, platoon ID, platoon depth by broadcasting beacon messages periodically. The platoon leader has a depth of 0, and it increases as we go farther. The leader acts as the coordinator and controls platoon decisions such as join/merge, split, leave, and dissolve. In this paper, We study two PMPs; since PLEXE [56] only specifies the join-at-tail maneuver that is the same as Join/Merge maneuver in VENTOS, we thus mainly follow the description of PMP in VENTOS [69].

Join/Merge Maneuver Two platoons, traveling in the same lane, can initiate a merge maneuver to form a bigger platoon. The leader of the rear platoon will send a `MERGE_REQ` to the front platoon leader, if it observes that the combined platoon size is no greater than the optimal platoon size by

inspecting the beacon message from front vehicles. Upon receiving a MERGE_ACCEPT from the front leader, the rear platoon leader will speed up to reduce the front spacing. Then, the rear leader sends CHANGE_PL to notify its followers to change the platoon leader to the front leader. Meanwhile, the rear leader switches to the follower role after sending a MERGE_DONE to the front platoon leader.

Split Maneuver To break the platoon into two smaller platoons, a platoon leader can either actively initiate this maneuver at a specific position, or passively trigger this maneuver when the platoon size exceeds the optimal platoon size. A platoon leader first sends a SPLIT_REQ to the splitting vehicle where the split should occur. After receiving a SPLIT_ACCEPT, the platoon leader sends a CHANGE_PL to make the splitting vehicle a potential leader. Besides, the platoon leader needs to inform followers behind the splitting vehicle, if any, to change their leader to the splitting vehicle. After that, the platoon leader sends a SPLIT_DONE to the splitting vehicle, which then switches to the leader role.

Leave Maneuver A platoon member may initiate a leave maneuver, when approaching the destination. For the leader leave, the leader will send a VOTE_LEADER to all followers to vote on the new platoon leader. The newly elected platoon leader needs to send a ELECTED_LEADER to the current leader. Then, the leader splits at the position of the elected leader by initiating the *split maneuver*, and thus hands over the leadership to the elected leader. For the follower leave, the follower will send a LEAVE_REQ to the leader and wait for a LEAVE_ACCEPT. The leader needs to split at both the succeeding vehicle, if any, of the follower, and the follower to make it a free agent, defined as a one-vehicle platoon. At this time, the follower can slow down. Once there exists enough space for the follower to change the lane, it will send a GAP_CREATED to the old leader and finally leave the platoon.

Dissolve Maneuver This maneuver is only initiated by the platoon leader, who broadcasts a DISSOLVE to all followers. Upon receiving all ACK messages, all platoon members act as free agents and are free to leave.

3 Threat Model

CV communication capability. In our work, we assume that the attacker can compromise OBUs on her own vehicles or others' vehicles, which follows recent works on CV security [14, 15, 74]. This assumption is reasonable, as previous works [13, 39] have already shown that in-vehicle systems can be compromised physically or remotely. In this case, the attacker can send malicious packets to other vehicles through compromised CV devices. All malicious packets should comply with protocol specifications. Notably, the attacker is allowed to unicast malicious packets to a specific vehicle (cf. IEEE 1609.3, Subclause 5.5.1).

Passive monitoring. The attacker can passively eavesdrop and capture all network traffic in her wireless communication range under the promiscuous mode of the wireless adapters.

Cryptography operations. We assume that cryptography operations used in CV protocols (e.g., signing, verification, and hash) are secure. The attacker thus cannot forge digital signatures used for packet authentications but can use valid certificates installed in compromised vehicles to sign outgoing packets. However, the attacker can still (1) passively collect valid certificates by sniffing the CV network traffic, and (2) construct local certificates, which are not signed by trusted anchors.

4 Analysis Methodology

In this section, we first present our how we construct each component in the model, including the adversary model and each protocol state machine. We then describe how we reduce the state space and document how we implement *CVAnalyzer*.

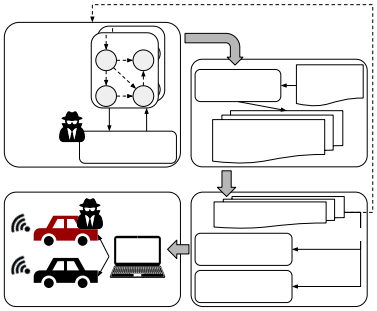

Figure 2: *CVAnalyzer* overview. (Events: (1) incoming/outgoing packets, (2) added/deleted/expired timers)

4.1 Model Construction

As shown in Figure 2, our model, consisting of the environment and protocol state machines ($\mathcal{P}$), is driven by network and timer events. In general, the environment manages packet/time events generated by protocol state machines. It delivers triggered events (e.g., packet reception, timeout) to protocol state machines.

Adversary-controlled communication environment. We follow the design in prior works [59] and define three sequential steps in a loop for the environment:

1. `Retrieve`: the environment picks one of many different packet/time events if such an event is available.
2. `Process`: the protocol state machine processes an event.
3. `PostProcess`: after processing a given event, the protocol state machine either sends a new packet, adds a new timer, cancels an existing timer, or does nothing. The environment needs to update its internal states and keeps track of newly added events.

Our threat model (§ 3) assumes that the attacker has communication and eavesdropping capabilities. Thus, we add one more step for the attacker to send and receive arbitrary packets:

4. `Attack`: the attacker is able to monitor all packets in the environment. If needed, she can inject arbitrary packets into the environment, which allows a protocol state machine to process all possible packet events.

To model the network, we construct the communication channel $\mathcal{C} = \{\mathbf{ch}_{i,j} | i, j \in [1,n], i \neq j\}$, where $\mathbf{ch}_{i,j}$ is a FIFO queue from $\mathcal{P}_i$ to $\mathcal{P}_j$. In this case, the packet sending and reception are abstracted as enqueue and dequeue operations on $\mathbf{ch}_{i,j}$. Notably, we do not consider network factors for vulnerability discovery, such as network latency and packet loss, because the lossy and erroneous network weakens the attack's capability and increases the complexity of the model. Placing the attacker in her best position can help us uncover all potential attacks. On the other hand, to model timers, we do not keep track of the absolute time but only care about the temporal ordering of events, which is a common practice in model checking distributed system [43]. For progress advancing, all timers will count down simultaneously if there are no active events that should be delivered to protocol state machines.

Protocol state machine. All protocol participants ($\mathcal{P}_i$, $i \in [1,n]$) are identical; therefore, each of them can be represented as the same finite-state machine (FSM). Then, our model $\mathcal{M}$ can be defined as a concurrent system $\mathcal{M} = \mathcal{C} || _{i \in [1,n]} \mathcal{P}_i$, including an adversary-controlled environment $\mathcal{C}$ and n isomorphic processes $\mathcal{P}_i$, where $||$ is commutative and associative.

In our analysis, we abstract the higher-layer protocols in the CV network stack: (1) the communication model defined in networking services and message sublayer, (2) security services, and (3) PMP described in [5, 56, 60, 69]. We follow their specifications or codebases to define packet and timer handlers, which update the internal states of $\mathcal{P}_i$ while processing packets and timeouts delivered by the environment. Our model excludes the handler of certificate revocation in security services, because it relies on an external public key infrastructure (PKI) like SCMS [12] to revoke certificates, which is out of the scope of the network stack itself. We will discuss how SCMS affects identified vulnerabilities in § 8.

For the security services, we first abstract away cryptographic constructs because we assume that the cryptography operations in CV protocols are secure. Then, we model both packet type and packet header data, as they are required by the internal security mechanisms. In CV network, each protocol participant will have a batch of unique end-entity certificates (a.k.a., signing certificates). To trigger all internal security mechanisms, for the certificate configuration, we assume that the issuer of each batch of signing certificates is different from each other and is attached with packets in transmission.

Probabilities. Network protocol involves many concurrent events (e.g., packet transmission), leading to concurrent transitions in state machines. While building probabilistic models, we develop a discrete-time Markov chain (DTMC) model that assigns uniform probabilities to concurrent state transitions, originating from the same state (§ 4.2).

State reduction. We now show how we abstract the model to reduce states through a concrete example. For ease of exposition, we rely on a simplified example (Figure 3) derived from `N4` (§ 5.1.3). Our goal is to reduce unnecessary states to get an abstracted model. Also, we want to ensure that *the counterexample found in the abstracted model is a valid counterexample in the original model.*

```
1  h(x) ≜ x%M  h(x) = x mod M
2  EventRange ≜ (0 .. (N − 1))
3  TimerIndexRange ≜ (0 .. (M − 1))
4  Init ≜  Initial state
5      ∧ event ∈ EventRange
6      ∧ timer = [i ∈ TimerIndexRange ↦ None]
7  Next ≜  Specify how to update states
8      ∧ event′ ∈ EventRange
9      ∧ timer′ = [i ∈ TimerIndexRange ↦
10         IF h(event) = i THEN TIMEOUT  initialize the timer
11         ELSE IF timer[i] = None THEN timer[i]  not initialized
12              ELSE IF timer[i] > 0 THEN timer[i] − 1  count down
13                   ELSE None]  expire
14 Property ≜
15     ∀ i ∈ TimerIndexRange :
16         (timer[i] = TIMEOUT) ⇝ (timer[i] = 0)
```

Figure 3: A simplified example derived from `N4` (`N`: the total number of events; `M`: the total number of timers; `TIMEOUT`: the maximum value of the timeout).

In the example, we develop a simplified protocol, in which the model updates the `timer` according to the `event` (Line 9-13), in which the function $h(x)$ abstracts the hash truncation operation in P2PCD. Assuming that, without the attacker, the range of *event* is $[0, X-1]$, where $X < M \leq N$. The attacker in the environment can trigger all possible events $[0, N-1]$.

For a given *event*, if $h(event)$ equals to i, then $timer[i]$ will be initialized (Line 10). For other unmatched timers, a timer will (1) remain unchanged if $timer[i]$ is not initialized (*None*), (2) count down if it has been initialized, or (3) set as uninitialized if it expires. To capture the attacker's behavior, for each *Next* step in Figure 3, we randomly select a value in *EventRange* as the next *event* (Line 8). Notably, events within $[X, N-1]$ are triggered by the attacker and can lead to the initialization of all timers. Last, to find counterexamples, we specify a liveness property (Line 14-16) that all timers should eventually expire if it has been initialized.

Obviously, the state space of the model depends on N and M, which can be arbitrarily large. For example, the timer index range in P2PCD would be $[0, 2^{24}-1]$ (i.e., $M = 2^{24}$). The number of events N can be 2^{256}. Unfortunately, the model checker cannot handle such large state space.

By analyzing the model, we observe that we do not need to track all $timer[i]$, as the protocol only updates a small set of timers when no attacker is presented. As stated before, without the attacker, the range of *event* is $[0, X-1]$; the model thus only updates $timer[i]$, where $i \in [0, X-1]$. Usually, the protocol instance does not care whether other timers can eventually expire. Therefore, apart from reducing *TimerIndexRange* to $[0, X-1]$, we also derive a weakened property, $\widehat{Prop}$:

$$\forall i \in [0, X-1] : (timer[i] = TIMEOUT) \rightsquigarrow (timer[i] = 0)$$

Since $\neg\widehat{Prop} \Rightarrow \neg Prop$, our decision ensures that if the identified counterexample violates $\widehat{Prop}$, it also violates $Prop$ and is a valid counterexample in the original model.

On the other hand, we observe that many events triggers the same update on $timer$. For example, both $event = 0$ and

$event = M$ leads to the initialization of $timer[0]$. Thus, we decide to keep a small set of $EventRange$. We first partition $EventRange$ into several equivalence classes:

$$EventRange_i = \{j \in EventRange | h(j) = i\}, i \in [0, M-1]$$

where every event in $EventRange_i$ triggers the same update on $timer[i]$. For each equivalence class $EventRange_i$, we then pick one value, $EventRange_i = \{i\}$, so that we can trigger all updates on $timer$. In this case, we reduce $EventRange$ to $[0, M-1]$. However, among this range, only events in $[X, M-1]$ is triggered by the attacker, meaning that the attacker itself cannot trigger all updates on $timer$. We thus enlarge $[X, M-1]$ to $[X, 2M-1]$ so that the attacker itself can trigger the initialization of all timers. Finally, we derive a small $\widehat{EventRange} = [0, 2M-1]$ and a mapping function:

$$f(x) = \begin{cases} x, & x \in [0, M-1] \\ M+i, & x \in \{j \cdot M + i | j \in [1, \lceil \frac{N}{M} \rceil - 1]\} \end{cases} (i \in [0, M-1])$$

Moreover, f is a surjective function; thereby, for every $\hat{x}$ in $[0, 2M-1]$, we can always find at least one x in $[0, N-1]$ such that $\hat{x} = f(x)$. In another word, for every identified counterexample in the abstracted model, we can always find at least one corresponding counterexample in the original model by applying the inverse function f^{-1} on $event$.

By combining the aforementioned two strategies together, we can successfully reduce the state space of the example and ensure no wrong property violations. In particular, we reduce $TimerIndexRange$ and $EventRange$ to $[0, X-1]$ and $[0, 2X-1]$ respectively.

4.2 Model Checking

The goal of using the general model checker is for vulnerability discovery. Given a model $\mathcal{M}$ and security properties, once the model violates a property, the general MC will generate a counterexample, an execution trace leading to the violation. Formally, a model can be defined as consisting in a finite set of states S, initial states $I \subseteq S$, the transition relation $T \subseteq S \times S$, and a labeling function from states to a finite set of atomic propositions $L : S \to 2^{AP}$ [17]. Table 1 summarizes the high-level properties to analyze P2PCD and PMPs. For each property, we first refine φ_i to get a new property $\varphi_i\prime$ such that $\varphi_i \Rightarrow \varphi_i\prime$ and $\neg\varphi_i\prime \Rightarrow \neg\varphi_i$. For example, a refinement over φ_1 would be *at least one CV device should eventually broadcast a learning request after observing an unknown certificate*. Then, MC is used to find property violations. By analyzing the counterexample, we can formulate the attack procedure (§ 5) and analyze the fundamental reasons for identified attacks, which is helpful for the mitigation design (§ 7). Last, we patch the model to ensure that the general MC will not generate the same type of violations later.

PMC aims at avoiding manual risk assessment and does not discard identified vulnerabilities from the general MC. It helps assess the severity of the exposed vulnerabilities and thus allows the protocol designers to prioritize the solution design. Unlike the general MC, PMC assigns probabilities for each state transition $T : S \times S \to [0, 1]$ such that

Table 1: Availability properties used by *CVAnalyzer*.

ID	Availability properties
φ_1	The application layer should be always able to consume valid incoming packets.
φ_2	Refinement over φ_1: All CV devices should eventually learn unknown certificates.
φ_3	Refinement over φ_1: All platoon members should eventually switch to idle state.

$\forall s \in S : \Sigma_{s\prime \in S} T(s, s\prime) = 1$. Since we assign uniform probabilities to concurrent state transitions, for all reachable successor states of s in $Succ_s = \{s\prime \in S | T(s, s\prime) > 0\}$, the transition probability between s and any $s\prime$ is $\frac{1}{|Succ_s|}$. A transition matrix can be derived from the transition probabilities. Thus, PMC can calculate the likelihood of transitioning from initial states to any target states. If we can formalize the states of the attack success, PMC can help us generate the attack success rate. Apart from the probability, PMC can also assign "time" costs for state transitions, which can be used to quantify time-related properties. In § 5, we leverage PMC to quantify the severity of non-deterministic attacks *N1-4*, which are defined as attacks that may not always succeed per attempt. We observe that, P2PCD attacks can succeed, *only if* malicious packets are delivered to the victim vehicle exactly within the attack time window. However, the attacker cannot precisely infer the start and end of the time window, but only roughly predict the start time. Thus, we use PMC to quantify their severity based on the success rate and the time delay.

4.3 Implementation

Following the proposed approach, to instantiate *CVAnalyzer*, we use TLC [75] as the general model checker due to its expressiveness of constructing the model, and pick PRISM [42] as our probabilistic model checker. As the prior step of model checking, we manually extract the abstract model of the IEEE 1609 protocol family [67] and PMPs [56, 69]. The abstract model includes two (i.e., $n = 2$) legitimate vehicles and one malicious vehicle (i.e., the attacker). Then, we need to implement concrete models in the modeling languages used by TLC and PRISM. As the supported maneuvers of PLEXE is a subset of VENTOS, we merge them together as one model. The properties that we want to verify in this paper are shown in Table 1 and Table 3, covering availability and quantitative properties respectively.

5 Analysis Results

In this section, we describe 4 DoS attacks in P2PCD and 15 attacks in VENTOS [69] and PLEXE [56] in detail (Table 2). Then, we analyze the security implications of identified attacks, and quantify the success rate and the average time delay in packet processing of those non-deterministic attacks.

5.1 P2PCD Vulnerabilities

In summary, *CVAnalyzer* finds 4 new DoS attacks that can compromise the availability of CV network. All 4 vulnerabilities come from P2PCD [32], which prevents victim vehicles from learning unknown certificates (see Figure 4). Without

Table 2: Summary of attacks found in the CV protocols. (**N**: CV network protocol, P2PCD. **A**: CV application, PMP)

ID	Name	Assumption	New?	Implications
N1	Response Mute	Known response threshold, optional response verification, enough computing power	Yes	Stop the CV device from sending learning responses; result in traffic accidents (§ 6.2.1)
N2	Request Mute	Optional response verification, enough computing power	Yes	Stop the CV device from sending learning requests; result in traffic accidents (§ 6.2.1)
N3		Known MAC address		
N4	Numb	Known MAC address	Yes	Stop the CV device from recording unknown certificates; result in traffic accidents (§ 6.2.1)
A1, *A2*	(Prerequisites)	Available platoon space	A1: No [1]. A2: Yes	Cause traffic collision [1], lead to *A3-15*
A3, *A4*	Split Trigger	Centralized platoon coordination	Yes	Interfere the traffic flow stability, decrease efficiency and safety (§ 6.2.2)
A5-14	PMP Block	-	Yes	Prevent platoon members from performing any maneuvers
A15	Inconsistency	Inappropriate validity check	Yes	Lead to failures of the split maneuver and the leader/follower leave maneuver

knowing necessary certificates, the victim vehicles cannot verify incoming packets; the CV network stack thus cannot deliver data to the application layer. Besides, we discuss the fundamental reasons for these vulnerabilities. Also, we assess their security consequences.

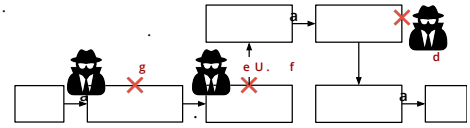

Figure 4: Four P2PCD attacks can break the whole pipeline of P2PCD learning process to prevent the CV device from learning/storing the unknown certificate.

In the following descriptions, two CV devices, `Vehicle 1` (`V1`) and `Vehicle 2` (`V2`), broadcast SPDUs every 100 *ms*. However, `V2` cannot verify packets sent by `V1` because `V2` does not know the issuer `ca1` of the signing certificate `ee1` used by `V1`. `V2` thus wants to learn the unknown certificate `ca1`. For each attack presented below, `V1` first sends a trigger SPDU to `V2`. In the normal case without the attacker, after receiving the trigger SPDU, `V2` initializes P2PCD learning process and attaches learning request information in the next outgoing SPDU. `V1` will construct and send the learning response after receiving the learning request.

5.1.1 Response Mute Attack

N1 can prevent a peer CV device from sending the learning response. This attack exploits the optional verification of learning responses and the throttling mechanism of P2PCD that limits the number of responses to a single request. The attacker intentionally interact with `V1` by sending multiple malicious learning responses to ensure that the response counter of `V1` exceeds the response threshold. As a consequence, `V1` choose not to send the learning response, and `V2` fails in learning the unknown certificate `ca1`.

Assumptions. For successfully carrying out this attack, the attacker needs to know the exact value of the response threshold. For example, the response threshold of BSM is 3 [20]. We assume that `V1` does not mandate the verification for incoming learning responses, which is consistent with the current protocol specification (§ 2.1). Also, we assume that the attacker has enough computing power to efficiently construct learning responses that can cause partial hash collision (e.g., low-order 3 bytes collision).

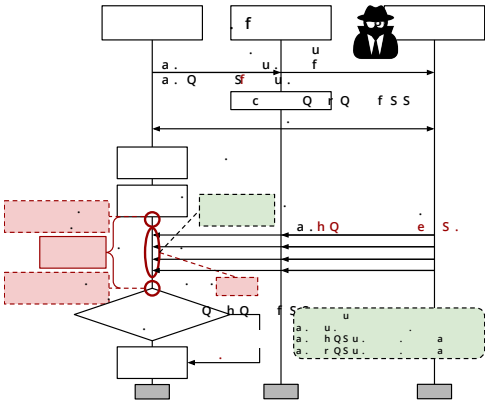

Figure 5: *N1*: the attacker can stop V1 from sending learning responses to V2 by sending multiple malicious learning responses.

Attack steps. Figure 5 illustrates the attack steps in detail. `V1` first sends a trigger SPDU to `V2`. Instead of immediately sending the learning request, `V2` stores the `HashedId8` value of the unknown certificate `ca1` in a queue (cf. IEEE 1609.2 [32], Subclause D.4.2.1.1). `V2` attaches the `HashedId3` value of `ca1` in the learning request field of its next outgoing SPDU. In P2PCD, `HashedId8` and `HashedId3` stands for the low-order 8-byte and 3-byte hash of a certificate respectively. After receiving the learning request, `V1` starts to prepare a learning response. Based on the throttling mechanism, `V1` initializes the response backoff timer and the response counter for the requested certificate.

However, the attacker can observe the trigger SPDU and the learning request, so she can determine that `V2` wants to learn an unknown certificate from `V1`. The attacker thus deliberately constructs multiple learning responses, in which the `HashedId3` value of the first certificate in the payload matches with the unknown certificate `ca1`. The attacker then sends out these malicious packets to saturate `V1`'s response counter (i.e., making it no less than the response threshold). On receiving malicious learning responses, `V1` wrongly updates its response counter (via `AddCertificate` primitive defined in IEEE 1609.2). When the response backoff timer expires, `V1` checks whether the response counter is less than

or equal to the response threshold. Obviously, based on the current status of the response counter, V1 decides to discard the response at this time.

Discussion. The reason for *N1* can be attributed to the use of truncated hash. By design, the hash function should be resistant to collision attacks. However, the use of truncated hash value compromises the security provided by the hash function. For example, for HashedId3 used in CV network (i.e., three-byte hash), collision could be found in the brute-force number of 2^{24}. Most importantly, the response counter uses HashedId3 as the identifier, which means that the attacker can manipulate the response counter if she constructs certificates leading to the partial hash collision. On the other hand, as introduced in § 2.1, IEEE 1609.2 does not mandate the verification for the learning response. Thus, it is still possible that some poorly implemented CV protocols may not verify the incoming learning response but just store certificates in the payload. Even if the CV device mandates the verification, the attacker can collect certificates with the attacker-desired hash values offline (§ 7). Note that, since P2PCD learning responses do not carry digital signatures, the attacker does not need to possess a legitimate certificate to launch *N1*, making the attack much more stealthy.

5.1.2 Request Mute Attack

Both *N2* and *N3* can stop CV device from sending learning requests. Similar to *N1*, *N2* exploits the hash collision issue. Readers can refer to §A for more details.

N3 exploits the unicast capability and injects a malicious SPDU with the same learning request field (i.e., the HashedId3 value of ca1) as what V2 intends to send. As a result, V2 can observe the malicious learning request and decides not to send its own learning request. V2 hence fails in learning unknown certificate ca1 because V1 does not receive any learning requests.

Assumptions. To successfully launch this attack, the only requirement is that the attacker needs to know the MAC address of the victim vehicle V2. This is reasonable because the attacker can monitor all traffic in the network; it can thus observe V2's MAC address from packets sent by V2.

Attack steps. As presented in Figure 6, V2 initializes P2PCD after receiving a trigger SPDU from V1. V2 stores the HashedId8 value of the unknown certificate ca1 in a queue. Meanwhile, since the attacker can observe the trigger SPDU, she constructs a malicious learning request, in which the learning request field m.lr equals to the HashedId3 value of the unknown certificate ca1. In P2PCD, after receiving a learning request, V2 removes any matching HashedId8 entries in the queue. Therefore, V2 removes the entry of the unknown certificate h8(ca1) in the queue, where h8 is a function to get the low-order eight-byte hash of the input. As the queue becomes empty, V2 decides not to attach the learning request information in the next outgoing SPDU. Consequently, V2 is unable to learn the correct unknown certificate.

Discussion. The fundamental reason for *N3* is that once a vehicle observes an active P2PCD learning request, it will not send the learning request for the same unknown certificate. In the normal case, this mechanism is helpful to reduce the number of simultaneous learning requests in the fly. However, the attacker can unicast the learning request to the victim vehicle. Notably, the attacker should not send such learning request to the owner of the unknown certificate (i.e., V1 in Figure 6). This attack misleads the victim vehicle to believe that some other legitimate vehicles are requesting the same unknown certificate. The protocol designers do not consider the use of unicast in P2PCD, which makes the victim vehicle vulnerable to *N3*. On the other hand, *N3* does not require the attacker to possess a legitimate certificate to sign the learning request but only uses self-generated certificates. As long as the digital signature of the learning request is valid, the vehicles will process the learning request field in the packet header. In this case, the signing certificate of the malicious learning request will be treated as an unknown certificate and will trigger another P2PCD learning process. Therefore, even if the certificates used by the attacker is revoked, the attacker can always generate new certificates for future use.

5.1.3 Numb Attack

First, like *N3*, this attack exploits the unicast capability and injects a malicious SPDU with the same learning request field (i.e., the HashedId3 value of ca1) as what V2 intends to send. This causes the same consequence as *N3*, in which V2 chooses not to send the learning request and thus cannot learn the unknown certificate. Then, due to the request active timer (e.g., reqActiveTimer), V2 still thinks that there should be an active request in the fly. Therefore, while receiving the next trigger SPDU, V2 chooses not to add the HashedId8 value of the unknown certificate ca1 into the queue and keeps waiting for learning responses.

Attack steps. As described in Figure 6, this attack is similar to *N3*, but the attacker has different attack goal that it tries to prevent the victim vehicle V2 from recording unknown certificates. Since V1 broadcasts BSMs every 100 ms, V2 will receive a trigger SPDU again in a few milliseconds. At this time, V2 still cannot verify the incoming packet. However, because the request active timer has been initialized in the last communication round, and the timer is usually set to 250 ms [20], V2 believes that there is still an active learning request in the fly. Thus, V2 does not add anything into the queue, which means that it will not attach any learning request information in the next outgoing SPDU. V2 cannot recover from this malicious state until the request active timer expires.

Discussion. *N4* has the same fundamental reasons as *N3*. The only difference is that the request active timer blocks the victim vehicle from recording unknown certificates in that the initial value (i.e., 250 ms) of the timer is around 3 times larger than the broadcast interval (i.e., 100 ms). Fortunately, P2PCD allows the user to configure the parameters for the

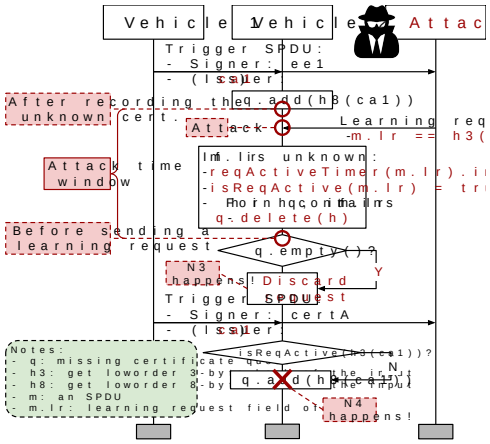

Figure 6: *N3* can stop V2 from sending learning requests to V1 by sending a malicious learning request.. *N4* can stop V2 from recording unknown certificates by sending one or more malicious learning requests.

initial value of timers.

Table 3: Quantitative properties used by *CVAnalyzer* to quantify the security consequences of *N1-4*

ID	Quantitative properties
ψ_1	What is the success rate of the attack?
ψ_2	What is the expected time delay of processing next SPDU?

5.1.4 Assessment

We observe that, *N1-4* can succeed, *only if* the attacker delivers the malicious packets to the victim vehicle exactly within the *attack time window*. However, one challenge for the attacker is that she cannot precisely determine the start or end of the *attack time window* but can only roughly estimate the time window. Thus, we are motivated to quantify the probability of successfully launching the attack by using the probabilistic model checker in *CVAnalyzer*.

Table 4: Attack assessment results of *N1-4*.

ID	Attack packet	Attack time window	Succ. Rate	Time delay (*ms*)
N1	RES-H3	0-250 ms	99.47%	580 (280 + 300)
N2	RES-H8	$\leq$ 100 ms	99.99%	370 (280 + 90)
N3&4	LR-H3	$\leq$ 100 ms	99.99%	570 (280 + 290)

Table 4 summarizes the quantification results. Since *N3* and *N4* use the same type of packet to attack the victim vehicles, and the *attack time window* of them are the same, we merge these two attacks together and quantify the probability results based on the type of *attack packet*.

For *N1*, the success rate is 99.47%. We set the response threshold as 3 in our experiments. To successfully launch one attack, the attacker has at least send 4 malicious learning responses, while the rest attacks only need to send one malicious packet. This is why the success rate of *N1* is slightly lower than other three attacks. For *N2-4*, the success rates are 99.99%. If V2 is able to send the learning request before receiving the malicious packet, the attacker will fail. However, this is unlikely to happen based on our results.

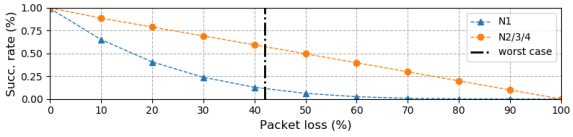

Figure 7: The success rate of *N1-4* under packet loss.

To have a deeper understanding how the network factor will affect the success rate, we leverage packet loss to demonstrate the capability of PMC. Figure 7 show that the success rate of *N1* decays much more than the other three attacks, because the attacker of *N1* needs to successfully send at least 4 malicious packets to ensure success. As *N2-4* target the same attack time window, they have the same success rate. For *N1-4*, the attacker should immediately launch the attack once the victim vehicle enters her communication range. Bai et al. [7] show that the packet loss rate (PLR) and the distance between two CV devices are positively correlated in real-world settings. In a freeway environment, the PLR is around 42% if two CV devices are 450*m* apart, in which 450*m* is the longest communication distance presented in their study. Thus, we highlight the success rate when the victim vehicle enters the attacker's communication range, which is the worst case for the attacker (PLR: 42%). Although the packet loss decreases the attack success rate, it also affects the transmission of normal packets, leading to the loss of critical CV safety packets.

Besides, CV communication is time-sensitive [2, 3, 25], so we would like to know the *time delay* caused by one round of *N1-4*, which is defined as the time duration from waiting for the trigger SPDU to successfully processing an SPDU from other vehicles. By knowing this, we can infer how long the CV network will recover from the attack if the attacker terminates attacking.

Table 4 shows that three of them can at least double the time delay in packet processing. During the experiments, we notice that there still exists *280 ms* time delay even if we disable the attacker, which is one-time delay introduced by P2PCD itself. For *N2*, the extra time delay introduced by the attacker is *90 ms*, around one broadcast interval, because the malicious learning response cancels out the learning request process triggered by the SPDU from V1. V2 thus needs to wait for next SPDU from V1, which takes one more round of broadcast interval. For *N1*, *N3*, and *N4*, the extra time delay caused by the attack is about *300 ms*. If the attacker stops attacking at some time, it takes around three broadcast intervals (i.e., 300 ms) for V2 to recover from DoS.

In *N1*, the extra time delay comes from the long processing time of P2PCD, due to the long time interval of the response backoff timer, with a random timeout value between 0 and 250 *ms*. As shown in Figure 5, the attacker sends malicious learning responses to V1 right after V1 initializing the response backoff timer. Since the attack occurs at a very late stage, all the time before the transmission of the learning request

become useless. Also, a new P2PCD learning process to the unknown certificate `ca1` will not be initialized again until both the response backoff timer of `V1` and the request active timer of `V2` expire. After that, `V2` needs to initialize P2PCD again; thus, one round of *N1* double the one-time delay of P2PCD. In *N3* and *N4*, `V2` is unable to process incoming trigger SPDUs until the request active timer expires. However, this timer is usually set to 250 ms, which largely increase the time delay.

5.2 PMP Vulnerabilities

CVAnalyzer identifies 15 attacks in the PMPs of VENTOS [69] and PLEXE [56] (see Table 2). Among identified vulnerabilities, *A1-4* are not directly related to availability issues but are building blocks of other attacks. Although the PMPs analyzed in this paper are academic prototypes, our main contribution is the verification methodology, which can be generally applied to future PMP protocols. Our results demonstrate the necessity of such a systematic verification methodology: using manual efforts, a very recent work [1] can only uncover 1 vulnerability (A1). In contrast, using *CVAnalyzer* for the same PMP implementation, we are able to automatically uncover not only the same one but also 14 more (A1-15), which demonstrates both substantially improved efficiency and effectiveness.

In the following descriptions, `V1` and `V2` still stand for vehicles. `V1` is a platoon leader, and `V2` is usually a follower. Their relative positions differ case by case.

5.2.1 PMP Attack Prerequisites

A1 and *A2* allow the attacker to become a valid platoon leader and follower. Abdo et al. [1] have demonstrated that *A1* can lead to the traffic collision and slow down the emergency vehicle. Although they do not directly cause security or safety breaches, we list *A1* and *A2* alone because they are prerequisites of other attacks. As described in §2.2, a platoon leader will send a merge request to a front platoon, if the combined platoon size is no greater than the optimal platoon size. Thus, the attacker can claim herself as a front platoon to take over another platoon or initiate a merge maneuver to join a platoon, leading to the success of *A1* or *A2* respectively.

5.2.2 Split Trigger Attacks

Both *A3* and *A4* (see §A for details on *A4*) can trigger the split maneuver at any positions. Without sacrificing her own speed stability, in *A3*, the attacker can further lead to a high-rate of vehicles entering and exiting a platoon, which decreases efficiency and safety [5].

Attack steps. In *A3*, the attacker first merges with `V1` as a malicious follower. Then, `V2` sends a `MERGE_REQ` to `V1` and join the platoon. At this time, the attacker intentionally sends a `LEAVE_REQ` with a wrong depth number of 2 to `V1`, in which the depth number indicates the splitting vehicle is `V2`. `V1` thus wrongly initiates the split maneuver at the position of `V2`. After the split process, `V2` receives beacon messages from the attacker and merges with the front platoon again, as described in §2.2. By repeatedly triggering merge and split maneuver of `V2`, the attacker downgrades the speed stability of `V2`.

Discussion. The reason for *A3* is that the platoon leader does not verify whether the platoon depth in the `LEAVE_REQ` matches with the sender ID or not. Usually, if the sender ID is related to unique signing certificates [32], it is difficult for the attacker to falsify the identity. However, the design of PMP uses the depth information as the identity, which can be easily modified by the attacker. Thus, PMP opens a door for the attacker to trigger the leave maneuver, leading to a split maneuver at arbitrary positions.

5.2.3 PMP Block Attacks

This is the most common type of vulnerabilities (*A5-14*) in the current PMP design of both VENTOS and PLEXE, which misleads the victim vehicle to stay at a busy state. We only describe *A7* here. Please refer to §A for more details on others.

Attack steps. In *A7*, the attacker first joins the platoon by launching *A2* and aims at blocking the split maneuver. Usually, only the platoon leader can initiate the split maneuver, but the platoon follower cannot. However, the attacker can leverage *A3* and *A4* to mislead the platoon leader to send a `SPLIT_REQ` to any specified platoon members. In *A7*, the attacker receives a `SPLIT_REQ` from `V1` but chooses not to reply with a `SPLIT_ACCEPT`. Thereby, the platoon leader will keep waiting for the split reply. At this time, if `V2`, which is ahead of the attacker, approaches the destination and wants to leave the platoon, the leader `V1` will not be able to process the leave request or manage the split process to create space for `V2`. Without enough space at the front and rear of the vehicle, it is dangerous for `V2` to directly change the lane.

Discussion. The fundamental reason for *A5-14* is the lack of error recovery mechanism on communication failures. By design, the CV network stack does not provide reliable communication; it is the applications' responsibility to handle communication failures [34]. Researchers have already discussed the impact of communication failures on the CACC controller [5, 47], but do not pay much attention to communication failures on PMP. Also, we observe that PMPs in both VENTOS and PLEXE do not consider "offline" platoon members; thus, they do not design any error recovery mechanisms to reset the vehicle's state. Although we understand the PMPs of VENTOS and PLEXE are research prototypes, identified *PMP block attacks* still emphasize the importance of error recovery mechanisms in CV application design.

5.2.4 Inconsistency Attack

This attack aims at assigning a wrong depth number to a victim follower, which is inconsistent with the index in the platoon member list. The platoon depth is used in the split maneuver, so the inconsistent depth number can lead to failures of the split maneuver and the leader/follower leave maneuver.

Attack steps. In this attack, the attacker first joins `V1`'s platoon as a follower. Then, the attacker slows down to create

large gap (e.g., 100 m) between herself and V1. At this time, V2 change its lane and drives behind V1. V2 receives the beacon message from V1 and sends a MERGE_REQ to V1. After merging with V1, V1 updates its local state by appending V2's ID to the platoon member list, indicating the real platoon depth of V2 is 2. However, V2 only receives a beacon message with the depth of 0 from the front vehicle V1; V2 thus wrongly sets its platoon depth to 1. At this time, the attacker sends a LEAVE_REQ to V1. Since, V1 thinks that the attacker is a middle follower, and V2 is behind the attacker, it sends a SPLIT_REQ to V2 to create rear space for the attacker. In VENTOS, we observe that CHANGE_PL does not present the absolute depth but carries the relative change of depth information, because it is convenient for the platoon leader to send all followers one CHANGE_PL rather than multiple different CHANGE_PL. During the split maneuver, V2 receives a CHANGE_PL from V1 with the depth change of -2. While updating the depth information locally, PMP of V2 throws an error for the invalid new depth: $1-2=-1$, which may compromise the availability of PMP, as well as terminates the split maneuver.

Discussion. The reason for *A15* can be attributed to the inconsistent platoon view on the platoon leader and follower. When joining a platoon, the vehicle relies on the depth information in the beacon message from the front vehicle to set its own depth number, while the platoon leader simply appends a new member to the platoon member list without checking the relative location information. If the front vehicle is a benign last follower, no inconsistency will appear; otherwise, any CHANGE_PL from the leader to the victim vehicle will lead to a wrong new depth number. However, the attacker can either create a large gap for the victim vehicle (*A11*), or can send a beacon message with a wrong depth number if the attacker is the last follower.

6 Evaluation

In this section, we conduct extensive experiments and answer the following three research questions:

- **RQ1**: Are identified vulnerabilities practical in a real-world setting?
- **RQ2**: What are the security/safety impact of identified vulnerabilities?
- **RQ3**: What is the runtime performance of *CVAnalyzer*?

6.1 RQ1: Practicality of Identified Attacks

We implement and validate all attacks from both P2PCD and PMP, detected by *CVAnalyzer*, in a real-world testbed, which thus concretely demonstrates the effectiveness of *CVAnalyzer*. Interestingly, we also find some poor implementation details in real-world CV devices that actually make our attacks easier.

6.1.1 Testbed Setup and Tool Preparation

As shown in Figure 8, we set up a CV network using three Cohda OBUs [19] in our lab. Among these three OBUs, denoted as OBU 1, 2, and 3 respectively, OBU 1 and 2 are used as victim CV devices, and OBU 3 is used as the attack device. To control the experiments, we connect a laptop with three OBUs via Ethernet connections.

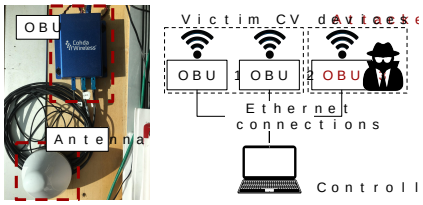

Figure 8: Testbed setup for attack validation.

The Cohda OBU that we use in our experiments is an ARM embedded device running Ubuntu 16.04. It implements the latest version of the CV network stack, which conforms with IEEE 802.11p [37, 38], IEEE 1609-2016 [32–34], and SAE J2735-2016 [20]. Notably, the implementation of IEEE 1609.2, called Aerolink, is developed by OnBoard Security [52] and closed source.

Victim OBU setup. To implement the CV communication model, both victim OBUs run a simple program that periodically broadcasts a correctly-signed SPDU. This broadcast-based communication also allows the attacker to observe all network traffic. For P2PCD, we place random data in the SPDU. For PMP, the SPDU stands for the beacon message, which contains the platoon ID and depth. Besides, both OBUs run PMP programs that are extracted from the source codes of VENTOS [69] and PLEXE [56].

For two different protocols (i.e., P2PCD, PMP), we assign different roles to OBU 1 and 2. In P2PCD attacks (i.e., *N1-4*), following the same assumption in §5.1, OBU 2 cannot verify packets sent by OBU 1 due to a missing certificate, so OBU 2 wants to initialize P2PCD to learn the unknown certificate from OBU 1. In PMP attacks (i.e., *A1-15*), by default, OBU 1 and 2 belong to the same platoon. OBU 1 and 2 are the platoon leader and the platoon follower respectively.

Tool preparation. To launch the attacks, we need to prepare tools that allow us to (1) parse and construct arbitrary packets and certificates, and (2) sign and verify CV network packets correctly. For (1), we use asn1c [71] to extract C data structures used by CV network services from ASN.1 modules in protocol specifications, and port platoon message types from the source codes of VENTOS and PLEXE. For (2), we follow IEEE 1609.2 to implement the signing and verification functionalities. We start from ECDSA APIs provided by OpenSSL 1.1.0j [53]. The elliptic curve and the hash function that we use with ECDSA is NIST P-256 and SHA-256, respectively. We cross-validate the correctness of our tools using APIs of Cohda CV network stack. The Cohda CV network stack can process packets and certificates generated by our tool without throwing any errors.

Certificate configurations. As *N1-4* require triggering P2PCD, we need to configure the pre-installed certificates in both victim OBUs to ensure that OBU 2 cannot construct a certificate chain while verifying packets sent by OBU 1. Both OBU 1 and 2 can correctly verify packets from OBU 3

(attacker). First, we use our certificate generator to construct a Root CV certificate, referred as `root`, which is trusted by all three OBUs. Then, we use `root` to issue two intermediate Certificate Authority (CA) certificates: `ca1` and `ca2`. We add both `ca1` and `ca2` to the local certificate database of OBU 1, but only add `ca2` to the database of OBU 2. To generate end-entity certificates for signing packets, we utilize `ieeeAcfGenerator` in Cohda SDK to issue two batches of certificates: `batch1` for OBU 1 and `batch2` for OBU 2. Each batch is an `Aerolink`-specific file and contains 20 end-entities certificates. Besides, we use `ca2` to issue another end-entity certificate `ee3` for the attacker so that OBU 1&2 can construct a valid certificate chain for packets sent by the attacker.

Apart from generating these normal certificates, we also need to construct certificates that can cause hash collisions. In *N1* and *N2*, the first certificate in the malicious learning response should match with the low-order 3-byte and 8-byte hash value of the unknown certificate respectively. We therefore use our certificate generator to construct two CA certificates: `ca1-h3` and `ca1-h8`, which can lead to 3-byte and 8-byte hash collision with `ca1`.

Attack programs. Following the attack processes in §5, we implement different attack programs. For each attack program, we set the start condition and the fail condition. The attack programs will stop only if the fail conditions are satisfied; otherwise, they will keep running. For P2PCD attacks, the attack fails if she observes any learning response from OBU 1. For example, the attack program for *N1* will send malicious learning responses after observing a learning request sent by OBU 2 (i.e., `Vehicle 2` in Figure 5). If it observes a learning response sent by OBU 1, the program will stop, which means that the attack fails. For PMP attacks, the attack fails if the victim platoon member can still finish the merge, split, leave, or dissolve maneuver.

6.1.2 Validation Results

In the real-world experiments, we find that all attacks from P2PCD and PMP are successfully validated. Interestingly, we further find that some implementation details in `Aerolink` can actually make P2PCD attacks, *N1* and *N2*, even easier and even block the CV communication indefinitely.

First, we observe that *N1* and *N2* can indefinitely block the P2PCD learning process. Based on our model-checking findings in §5.1, once the adversary stops sending malicious learning responses, the victim devices should eventually be able to recover from DoS. However, in our real-world experiments, we find that even after the attack program terminates, OBU 2 still cannot learn the correct unknown certificate from OBU 1. After analyzing the execution log, we find that OBU 1 keeps sending the fake certificate (i.e., `ca1-h3`), while OBU 2 sends learning requests for the unknown certificate `ca1` to OBU 1. By design, a CV device responds to an incoming learning request only if the learning request field matches with a signing certificate which is recently used by that device. With the help of a binary disassembler called `Hopper` [11], we find that `Aerolink` actually does not check whether the certificate used for a learning response is indeed a recently used certificate. For example, in *N1*, OBU 1 stores the fake certificate (i.e., `ca1-h3`) carried by the malicious learning response from the attacker. Thus, during the preparation of the future learning response, OBU 1 has two candidates, `ca1` and `ca1-h3`, as they have the same low-order three-byte hash. When receiving learning requests, OBU 1 always picks `ca1-h3` and sends it to OBU 2, which thus permanently prevents OBU 2 to learn the correct certificate.

Second, to launch *N1*, we find that the attacker only needs to send 3 malicious learning responses instead of 4. Before running real-world experiments, we first measure the response threshold in `Aerolink`, and find that the threshold set in `Aerolink` is actually 2 instead of 3 in the protocol specifications. This finding is also confirmed using `Hopper`. In this case, the attacker only needs to send 3 malicious responses to succeed. Although this may not be a big improvement for the attacker, it still uncovers an implementation choice in `Aerolink` that is unexpectedly favorable to the attacker.

Third, we find that *N2* only requires 3-byte hash collision rather 8-byte hash collision, which largely lowers the bar of launching *N2*. In P2PCD, by design, a CV device records an unknown certificate by adding the identity of that certificate (i.e., an 8-byte hash value) into a queue. If the 8-byte hash of a certificate in an incoming learning response matches with any entries in the queue, that entry will be removed. To launch *N2*, the attacker has to intentionally cause the 8-byte hash collision to let the victim CV device wrongly remove an entry in the queue. However, according to our binary analysis through `Hopper`, we find that `Aerolink` actually uses a 3-byte hash of the unknown certificate to record its status. Therefore, in our real-world experiments, we use `ca1-h3` in *N2*, and the results further validates this finding. Later in §7, we will show why this small truncated hash (e.g., 3-byte hash) is not secure enough. Although the protocol specification does not clearly state how to record unknown certificates, Annex D in IEEE 1609.2 [32] gives an example of P2PCD implementation that uses the 8-byte hash as the identity to record the unknown certificate. Also, while recording the unknown certificate, the most complete identity about the unknown certificate is the 8-byte hash value. A CV network implementation should always use complete information rather than truncated information.

6.2 RQ2: Attack Impact

The following two case studies demonstrate the impact of identified attacks: (1) P2PCD attacks can lead to traffic accidents, which eliminates the benefits of V2V safety applications (e.g., Forward Collision Warning (FCW)); (2) PMP attacks can affect the speed stability of the victim vehicle.

Simulator setup. To evaluate the impact of identified attacks, we use a simulator, VENTOS (VEhicular NeTwork Open Simulator) [69], so that we can demonstrate the driv-

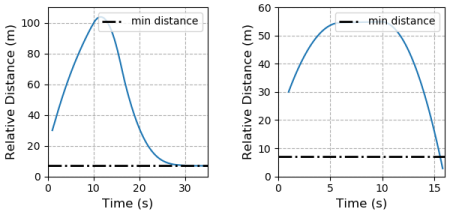

(a) No collision, FCW (b) Collision

Figure 9: Relative distance between the leading vehicle (V1) and the following vehicle (V2).

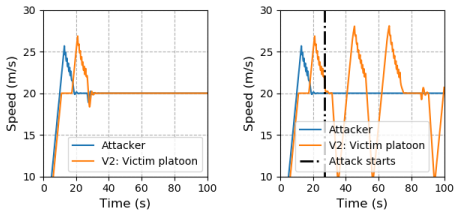

(a) Before attack (b) After attack

Figure 10: Speed profiles in *A3* (split trigger attack).

ing behavior under attacks. VENTOS is built upon SUMO road traffic simulator [62] and OMNeT++ [51]/Veins [61, 68] network simulator. These simulators [51, 62, 68] have been widely used in academia, industry, and the government. We configure it to use the models for the IEEE 802.11p [37] protocol for CV communication. Based on our reverse engineering and study on Aerolink (§ 6.1), we port the digital signature and P2PCD in IEEE 1609.2 to the simulator to secure BSMs and PMP commands. All secured packets are then transmitted through Wave Short Message Protocol (WSMP) and are directly sent to the data-link layer which uses continuous channel access based on IEEE 1609.4 [33].

Table 5: Vehicle parameters in the rear-end collision scenario.

Vehicles	Initial Speed	Max. Speed	Max. Decel.	Length
Leader (V1)	30 m/s	30 m/s	5 m/s^2	10 m
Follower (V2)	20 m/s	30 m/s	2 m/s^2	5 m

6.2.1 Safety Impact

By design, the CV safety application promises to increase personal safety [63]. However, our experiment results show that P2PCD attacks can fully eliminate the benefits of CV applications (e.g., Forward Collision Warning (FCW)), violating the original goal of CV applications.

Rear-end collision scenario w/ FCW. We first set up a rear-end collision scenario and demonstrate that vehicles with Forward Collision Warning (FCW), a V2V safety application, can avoid the accident (Figure 9a). The rear-end collision scenario includes a leading vehicle (V1) and a following vehicle (V2) with the initial parameters in Table 5. FCW alerts the driver in order to help avoid the severity of crashes into the rear end of other vehicles on the road [63]. We follow the FCW's design in Cohda SDK to actively monitor the distance between two vehicles. Once the distance is smaller than the safe distance, FCW will warn the driver. As FCW does not directly control the vehicle, after receiving FCW warnings, we ask the simulated vehicle to maintain a safe speed. Notably, we leverage Krauss car-following model [40], which is collision-free, to calculate the safe distance and safe speed.

During the simulation, both vehicles drive in the same lane. By exchanging BSMs, they can monitor each other's speed, position, and acceleration. The initial distance between two vehicles is 30 m, which is smaller than the safe distance at that time, thus triggering FCW. After starting the simulation for 10 s, V1 suddenly stops at the maximum deceleration (i.e., 5 m/s^2). Figure 9a shows that, before 10 s, V2 keeps increasing the distance to the leading vehicle due to the FCW. Therefore, after the leading vehicle suddenly decelerates, V2 has enough space to slow down safely.

Vehicles w/ FCW under attacks. Then, we place an attacker on the roadside who follows § 5.1 to launch P2PCD attacks and aims at causing traffic accidents, leading to a rear-end collision shown in Figure 9b. At the beginning of the simulation, both vehicles launch P2PCD to exchange certificates so that they can verify and process following BSMs. However, P2PCD attacks prevent them from learning certificates, meaning that they cannot process any BSMs from the peer vehicle. During the simulation, we observe that FCW is never triggered, so V2 accelerates to the maximum speed and follow V1. At 10 s, V1 starts decelerating at the maximum deceleration (i.e., 5 m/s^2). Since two vehicles are too close to each other (i.e., 54 m), and the maximum deceleration of the V2 is 2 m/s^2, V2 eventually collides into the rear end of V1.

6.2.2 Traffic Efficiency Impact

By design, CACC aims at increase traffic throughput and improve traffic flow stability [46, 57, 72]. However, *A3* and *A4* can interfere with the traffic flow stability, even without sacrificing her own speed stability, which violates the design goals of CACC. We place V1, the attacker, and V2 sequentially in the same lane and follow the attack steps of *A3* to run the simulation for 100 seconds. Figure 10 presents the speed profiles of V2, the victim platoon. In the normal case (Figure 10a), all vehicles will eventually reach a stable speed of 20 m/s; after launching the attack starting around time 27 seconds, we increase the standard deviation of V2's speed by 43%, further disturbing the following traffic.

6.3 RQ3: Performance of *CVAnalyzer*

Table 6 presents the runtime performance of *CVAnalyzer*. We run *CVAnalyzer* on a server with four 2.60GHz (8-core) CPUs and 128G memory. *CVAnalyzer* first explores all reachable states and then verifies given properties. Notably, without applying the state reduction, these two model checking tasks will take too long to explore reachable states. The results highlight the importance and effectiveness of state reduction.

Table 6: Runtime statistics of *CVAnalyzer*.

Attacks	Distinct States	Model Checking Duration
P2PCD	2209351	16s
PMP	142133161	1h 35min

7 Defense Proposals

Based on the discussions from previous sections, we propose defense solutions at the protocol design level:

1. Mandate verification for all learning responses;
2. Increase the truncated hash size for the issuer field in the certificate and the learning request field in SPDU;
3. Disallow unicast learning requests;
4. Bind the sender identity with the CV certificate;
5. Track platoon configuration data locally or remotely;
6. Design and integrate an error recovery mechanism.

Defense against N1 and N2. Solution 1 and 2 are proposed for *N1* and *N2*. Solution 1 by nature prevents *N1* and *N2* with local certificates. However, such solution can be evaded if attackers are still able to collect legitimately signed certificates with the attacker-desired hash values by sniffing CV network traffic. As estimated in Table 7, as long as the attacker can collect over 12000 different certificates, she can almost guarantee (>98% probability) that she can always have a certificate ready for triggering a 3-byte hash collision, which thus allow her to still launch *N1* and *N2* in real time. Collecting this many different certificates is completely realistic, considering that such collection process can be done offline. In addition, the collection process can also be greatly accelerated since the attacker can actively broadcast learning requests to trigger surrounding vehicles to return certificates with desired hash values, and also can place multiple attack devices in different locations to parallelize the collection process.

Table 7: Number of hash values needed for hash values of n-bits to cause a hash collision probability at p.

Number of hash values (k)					
Prob. of hash collision (p)	Number of bits of the hash value (n)				
	24	64	80	256	512
0.5	4823	5.06^{9}	1.29^{12}	4.01^{38}	1.36^{77}
0.99	12431	1.30^{10}	3.34^{12}	1.03^{39}	3.51^{77}

Solution 2 aims at increasing the difficulty of causing a hash collision, the key enabler for *N1* and *N2*. As shown in Table 7, it will be much more difficult for the attacker either to compute or to gather proper malicious learning responses. However, this will increase the DSRC packet size and thus may decrease the network performance, e.g., increasing network latency. We have reached out to the protocol developer, and confirmed that it is indeed a design choice to reduce the DSRC packet size. Thus, when applying Solution 2, the new size of the truncated hash type needs to be carefully chosen to balance such trade-off between security and protocol performance.

From our discussion above, neither solution 1 or 2 can fully eliminate the attack possibilities for *N1* and *N2*. Thus, to maximize the chance of preventing the attack in practice, the best choice would be using them jointly.

Defense against N3 and N4. Solution 3 is proposed for *N3* and *N4*, which thwarts both attacks by making it impossible to unicast the malicious learning request to block the P2PCD process. However, the down side is that this may break designed usage of unicast-based learning request. For example, as specified in IEEE 1609.0-2019 [36], CV applications will decide whether to use either unicast or broadcast, while receiving advertised services. Systematically understanding this trade off requires surveying and quantifying the demands of unicast-based learning requests at the CV application level, which we leave as future work.

Defense against A3. Solution 4 can prevent the attacker from triggering the split maneuver at arbitrary positions, but cannot stop her splitting succeeding platoon members. The certificate defined in IEEE 1609.2 [12, 32] provides a unique identity for each CV device. Safety-critical CV applications like PMP should always use unique and secure identities (e.g., certificates) rather than using self-defined identity (e.g., depth number), which is easily spoofed by the attacker. However, the attacker can still send a `LEAVE_REQ` to split at the succeeding vehicle and herself, which is a designed follower-leave behavior. The attacker can then join back to the platoon and launch the attack repeatedly. To completely address *A3*, we may require the assistant of misbehavior detection [12]. For example, a vehicle that keeps leaving and joining a platoon is highly suspicious. Designing an effective misbehavior detection requires comprehensively characterizing malicious behaviors, which we leave as future work.

Defense against A4 and A15. Solution 5 aims at eliminating wrong and inconsistent platoon information caused by *A4* and *A15*. In centralized PMP, a platoon leader is responsible for passing platoon configuration data to the new leader, when it leaves the platoon. The new leader can only accept the information from the old leader because it does not store any platoon configuration data. The design goal of the centralized PMP is to improve coordination efficiency and to enhance privacy because followers dynamically enter and exit the platoon [5]. However, the centralized design sacrifices the security, as a malicious leader can provide wrong platoon configuration data. To address *A4* and *A15*, on one hand, the platoon members can maintain a local copy of platoon configurations. On the other hand, RSUs can also provide services to remotely assist platoon members for tracking platoon configurations and guarding PMP commands [1]. As RSUs are often deployed and managed by trustworthy authorities, platoon members can rely on the infrastructures to correct wrong or inconsistent information.

Defense against A5-14. Solution 6 is straightforward and proposed for all PMP block attacks. As we mentioned before, CV applications should design their own error recovery mechanisms. With the error recovery mechanism, PMP should be able to recover from continuous packet loss. For example, PMP can define the retransmission and timeout threshold to avoid hanging at specific states. Apart from the classic solu-

tion to communication failures, it's worthing noting that PMP should also adjust the intra-platoon spacing between the "offline" member and the trailing platoon members accordingly to avoid traffic collision. If necessary, the platoon leader can dissolve the platoon and falls back to ACC mode.

8 Related Work

CV security analysis. Since the idea of VANET (i.e., the original idea of CV) has been around for more than ten years, many researches have already studied general threats to CV network [4, 28, 29, 44, 55, 55, 73]. However, as discussed in §1, existing works generally suffer from three limitations: (1) rely on manual inspection to identify potential threats [44, 55, 73], as opposed to automatic discovery in our work, (2) focus on security properties such as integrity, confidentiality, and privacy, as opposed to availability in our work, and (3) focus on prior generations of protocols or are conducted before the standardization of IEEE 1609 [4, 29, 44, 55, 73], as opposed to the latest version studied in our work.

Model checking security protocols. Model checking is a mature formal verification technique for finite state concurrent systems, and has been applied to several complex network protocols [22, 26, 30, 48, 50]. These works aim at exposing vulnerabilities in network protocols but does not consider quantitative assessments. *CVAnalyzer* can finish the attack discovery and the quantitative threat assessment without touching implementation details. Therefore, *CVAnalyzer* can be used by the protocol designer to evaluate the correctness of the protocol and also understand the severity of identified attacks, which can further guide the design of mitigation solutions. Also, this can largely minimize the cost to fix vulnerabilities, as all problems can be solved at the early stage.

Secure membership management. For a wireless ad-hoc network, a secure membership management system is necessary. Usually, network nodes form a peer group to share data with each other [49, 58, 76], and a group leader or other trusted entity is responsible for membership management. Wagner et al. [70] designed a decentralized blockchain-based system membership management for the platoon, in which each platoon member maintains a local copy of the blockchain, storing platoon information; however, it has scalability issues.

Due to the high mobility, the latest CV network does not form different communication groups, but adopts the digital signature (ECDSA), with the support of a PKI system, SCMS [12], to secure the communication. Any CV devices with valid certificates can broadcast data to others. To manage membership, the recently deployed SCMS [12] introduces misbehavior detection to identify malicious or malfunctioning members and then revoke their certificates. For our attacks, the certificate revocation in existing SCMS cannot prevent P2PCD attacks but can mitigate PMP attacks. The learning response in *N1* and *N2* does not require any signing certificates, so the certificate revocation cannot prevent the attacker from launching these two attacks. In *N3* and *N4*, the attacker can always generate new syntax-valid certificates for the learning request (i.e., an SPDU). Since the vehicle cannot distinguish the self-generated certificates with unknown certificates, the learning request field will still be processed. Unless the vehicle can always connect to the PKI (through RSU) to check the validity of unknown certificates, it is impossible to prevent the attacker from using self-generated certificates in the current CV network stack. Unfortunately, communication with the infrastructure may not always be present due to the deployment difficulties. We admit that if the PKI supports the online certificate status check, with the infrastructure coverage increase, the impact of P2PCD attacks will be diminished.

9 Conclusion

In this paper, we presents *CVAnalyzer* that harnesses the attack discovery capability of the general model checker and the quantitative threat assessment of the probabilistic model checker to automate the analysis. *CVAnalyzer* successfully detects 4 new DoS attacks in P2PCD and 15 attacks in PMP; also, we construct practical exploits and validate them in a real-world testbed. We have reported 4 P2PCD attacks to IEEE 1609 Working Group [35] and received confirmations. Also, we discuss the fundamental reasons for these vulnerabilities and propose effective mitigation solutions.

Future work. In the future, we would like to extend *CVAnalyzer* to verify more security properties, such as unlinkability. Though we only inspect the availability property in this paper, *CVAnalyzer* is actually general and can be extended to improve the verification capabilities. On the other hand, *CVAnalyzer* can be also extended to support other protocols in the context of CV (e.g., SCMS [12]). Also, we would like to improve the usability of *CVAnalyzer*. For example, we can introduce an intermediate representation for the model that can be automatically converted into the modeling language used by different model checkers. Therefore, we do not need to write the model twice for two different model checkers.

Acknowledgments

We would like to thank Yulong Cao, David Ke Hong, Yuru Shao, and the anonymous reviewers for providing valuable feedback on our work. This research was supported in part by an award from Mcity at University of Michigan, and by the National Science Foundation under grant CNS-1930041, CNS-1526455, CNS-1850533 and CNS-1929771.

References

[1] A. Abdo, S. M. B. Malek, Z. Qian, Q. Zhu, M. Barth, and N. B. Abu-Ghazaleh. Application level attacks on connected vehicle protocols. In *Proc. RAID*, 2019.

[2] F. Ahmed-Zaid, F. Bai, S. Bai, C. Basnayake, B. Bellur, S. Brovold, G. Brown, L. Caminiti, et al. Vehicle safety communications–applications (vsc-a) final report. Technical report, 2011.

[3] F. Ahmed-Zaid, F. Bai, S. Bai, C. Basnayake, B. Bellur, S. Brovold, G. Brown, L. Caminiti, et al. Vehicle Safety Communications–

Applications (VSC-A) Final Report: Appendix Volume 1 System Design and Objective Test. Technical report, 2011.

[4] F. Ahmed-Zaid, F. Bai, S. Bai, C. Basnayake, B. Bellur, S. Brovold, G. Brown, L. Caminiti, et al. Vehicle Safety Communications–Applications (VSC-A) Final Report: Appendix Volume 3 Security. Technical report, 2011.

[5] M. Amoozadeh, H. Deng, C. Chuah, H. M. Zhang, and D. Ghosal. Platoon management with cooperative adaptive cruise control enabled by VANET. *Vehicular Communications*, 2015.

[6] K. R. Apt and D. Kozen. Limits for automatic verification of finite-state concurrent systems. *Inf. Process. Lett.*, 1986.

[7] F. Bai and H. Krishnan. Reliability analysis of DSRC wireless communication for vehicle safety applications. In *IEEE ITSC*, 2006.

[8] D. A. Basin, C. Cremers, and C. A. Meadows. Model checking security protocols. In *Handbook of Model Checking*. 2018.

[9] D. A. Basin, J. Dreier, L. Hirschi, S. Radomirovic, R. Sasse, and V. Stettler. A formal analysis of 5g authentication. In *Proc. ACM CCS*, 2018.

[10] J. Bellardo and S. Savage. 802.11 denial-of-service attacks: Real vulnerabilities and practical solutions. In *Proc USENIX Security*, 2003.

[11] V. Bénony. Hopper. https://www.hopperapp.com/, 2019.

[12] B. Brecht, D. Therriault, A. Weimerskirch, W. Whyte, V. Kumar, T. Hehn, and R. Goudy. A security credential management system for V2X communications. *IEEE Trans. Intelligent Transportation Systems*, 2018.

[13] S. Checkoway, D. McCoy, B. Kantor, D. Anderson, H. Shacham, S. Savage, K. Koscher, A. Czeskis, F. Roesner, and T. Kohno. Comprehensive experimental analyses of automotive attack surfaces. In *Proc. USENIX Security*, 2011.

[14] Q. A. Chen, Y. Yin, Y. Feng, Z. M. Mao, and H. X. Liu. Exposing congestion attack on emerging connected vehicle based traffic signal control. In *Proc. NDSS*, 2018.

[15] Q. A. Chen, Y. Yin, Y. Feng, Z. M. Mao, and H. X. Liu. Vulnerability of Traffic Control System Under Cyber-Attacks Using Falsified Data. In *Transportation Research Board 2018 Annual Meeting (TRB)*, 2018.

[16] A. Cimatti, E. M. Clarke, E. Giunchiglia, F. Giunchiglia, M. Pistore, M. Roveri, R. Sebastiani, and A. Tacchella. NuSMV 2: An opensource tool for symbolic model checking. In *Proc. CAV*, 2002.

[17] E. M. Clarke, O. Grumberg, S. Jha, Y. Lu, and H. Veith. Progress on the state explosion problem in model checking. In *Informatics*, 2001.

[18] E. M. Clarke, W. Klieber, M. Novácek, and P. Zuliani. Model checking and the state explosion problem. In *LASER Summer School on Software Engineering*, 2011.

[19] Cohda Wireless. Mk5 obu. https://tinyurl.com/y6qepj6h, 2019.

[20] C.-C. T. Committee. Dedicated short range communications (dsrc) message set dictionary™ set. *SAE International*, Mar. 2016.

[21] D. L. Dill. The mur*phi* verification system. In *Proc. CAV*, 1996.

[22] M. Eian and S. F. Mjølsnes. A formal analysis of IEEE 802.11w deadlock vulnerabilities. In *Proc. IEEE INFOCOM*, 2012.

[23] J. Erickson, S. Chen, M. Savich, S. Hu, and Z. M. Mao. Commpact: Evaluating the feasibility of autonomous vehicle contracts. In *Proc. IEEE VNC*, 2018.

[24] ETSI. Telecommunications and Internet Protocol Harmonization Over Networks (TIPHON) Release 4; Protocol Framework Definition; Methods and Protocols for Security; Part 1: Threat Analysis. *Technical Specification ETSI*, 2003.

[25] J. Harding, G. Powell, R. Yoon, J. Fikentscher, C. Doyle, D. Sade, M. Lukuc, J. Simons, and J. Wang. Vehicle-to-Vehicle Communications: Readiness of V2V Technology for Application. Technical report, 2014.

[26] C. He and J. C. Mitchell. Analysis of the 802.11i 4-way handshake. In *Proc. WiSec*, 2004.

[27] G. J. Holzmann. The model checker SPIN. *Trans. Software Eng.*, 1997.

[28] H. Hsiao, A. Studer, C. Chen, A. Perrig, F. Bai, B. Bellur, and A. Iyer. Flooding-resilient broadcast authentication for VANETs. In *Proc. MobiCom*, 2011.

[29] Y. Hu, A. Perrig, and D. B. Johnson. Packet leashes: A defense against wormhole attacks in wireless networks. In *Proc. INFOCOM*, 2003.

[30] S. Hussain, O. Chowdhury, S. Mehnaz, and E. Bertino. Lteinspector: A systematic approach for adversarial testing of 4g lte. In *Proc NDSS*, 2018.

[31] IEEE 1609 WG. Ieee standard for wireless access in vehicular environments (wave) - networking services. *IEEE Std 1609.3-2010 (Revision of IEEE Std 1609.3-2007)*, 2010.

[32] IEEE 1609 WG. IEEE Standard for Wireless Access in Vehicular Environments–Security Services for Applications and Management Messages. *IEEE Std 1609.2-2016 (Revision of IEEE Std 1609.2-2013)*, 2016.

[33] IEEE 1609 WG. Ieee standard for wireless access in vehicular environments (wave) – multi-channel operation. *IEEE Std 1609.4-2016 (Revision of IEEE Std 1609.4-2010)*, 2016.

[34] IEEE 1609 WG. Ieee standard for wireless access in vehicular environments (wave) – networking services. *IEEE Std 1609.3-2016 (Revision of IEEE Std 1609.3-2010)*, 2016.

[35] IEEE 1609 WG. 1609 WG - DSRC Working Group. https://tinyurl.com/y2qju2t5, 2017.

[36] IEEE 1609 WG. Ieee guide for wireless access in vehicular environments (wave) architecture. *IEEE Std 1609.0-2019 (Revision of IEEE Std 1609.0-2013)*, 2019.

[37] IEEE 802.11 WG. Ieee standard for information technology– local and metropolitan area networks– specific requirements– part 11: Wireless lan medium access control (mac) and physical layer (phy) specifications amendment 6: Wireless access in vehicular environments. *IEEE Std 802.11p-2010 (Amendment to IEEE Std 802.11-2007)*, 2010.

[38] IEEE 802.11 WG. Ieee standard for information technology–telecommunications and information exchange between systems local and metropolitan area networks–specific requirements part 11: Wireless lan medium access control (mac) and physical layer (phy) specifications. *IEEE Std 802.11-2012 (Revision of IEEE Std 802.11-2007)*, 2012.

[39] K. Koscher, A. Czeskis, F. Roesner, S. Patel, T. Kohno, S. Checkoway, D. McCoy, B. Kantor, D. Anderson, H. Shacham, and S. Savage. Experimental security analysis of a modern automobile. In *Proc. IEEE S&P*, 2010.

[40] S. Krauß. Towards a unified view of microscopic traffic flow theories. *IFAC Proceedings Volumes*, 1997.

[41] H. Krishnan and A. Weimerskirch. "verify-on-demand"-a practical and scalable approach for broadcast authentication in vehicle-to-vehicle communication. *SAE International Journal of Passenger Cars-Mechanical Systems*, 2011.

[42] M. Z. Kwiatkowska, G. Norman, and D. Parker. PRISM 4.0: Verification of probabilistic real-time systems. In *Proc. CAV*, 2011.

[43] L. Lamport. Real time is really simple. *Microsoft Research*, 2005.

[44] C. Laurendeau and M. Barbeau. Threats to security in DSRC/WAVE. In *Proc. ADHOC-NOW*, 2006.

[45] J. Liu, D. Ma, A. Weimerskirch, and H. Zhu. Secure and Safe Automated Vehicle Platooning. *IEEE Reliability Society*, 2016.

[46] H. Mahmassani, H. Rakha, E. Hubbard, D. Lukasik, et al. Concept development and needs identification for intelligent network flow optimization (inflo) : assessment of relevant prior and ongoing research. Technical report, 2012.

[47] H. Mahmassani, H. Rakha, E. Hubbard, D. Lukasik, et al. Concept development and needs identification for intelligent network flow optimization (inflo) : concept of operations. Technical report, 2012.

[48] J. C. Mitchell, V. Shmatikov, and U. Stern. Finite-state analysis of SSL 3.0. In *Proc. USENIX Security*, 1998.

[49] S. Mäki, T. Aura, and M. Hietalahti. Robust membership management for ad-hoc groups. 2000.

[50] P. Narayana, R. Chen, Y. Zhao, Y. Chen, Z. Fu, and H. Zhou. Automatic vulnerability checking of ieee 802.16 WiMAX protocols through TLA+. In *Proc. IEEE Workshop on NPSec*, 2006.

[51] OMNeT++. Omnet++ simulator. https://omnetpp.org/, 2020.

[52] OnBoard Security. Aerolink secure vehicle communication. https://tinyurl.com/yaklyx47, 2019.

[53] OpenSSL. Openssl. https://www.openssl.org/, 2019.

[54] J. Petit, F. Schaub, M. Feiri, and F. Kargl. Pseudonym schemes in vehicular networks: A survey. *IEEE Comm. Surveys & Tutorials*, 2015.

[55] J. Petit and S. E. Shladover. Potential cyberattacks on automated vehicles. *IEEE Trans. Intelligent Transportation Systems*, 2015.

[56] PLEXE. The platooning extension for veins. plexe.car2x.org, 2019.

[57] J. Ploeg, B. T. M. Scheepers, E. van Nunen, N. van de Wouw, and H. Nijmeijer. Design and experimental evaluation of cooperative adaptive cruise control. In *Proc. ITSC*, 2011.

[58] M. K. Reiter, K. P. Birman, and L. Gong. Integrating security in a group oriented distributed system. In *Proc. IEEE S&P*, 1992.

[59] S. Resch and M. Paulitsch. Using TLA+ in the development of a safety-critical fault-tolerant middleware. In *Proc. ISSRE*, 2017.

[60] M. Segata, S. Joerer, B. Bloessl, C. Sommer, F. Dressler, and R. L. Cigno. Plexe: A platooning extension for veins. In *Proc. VNC*, 2014.

[61] C. Sommer, R. German, and F. Dressler. Bidirectionally coupled network and road traffic simulation for improved IVC analysis. *IEEE Trans. Mob. Comput.*, 2011.

[62] SUMO. Simulation of Urban MObility. https://sumo.dlr.de, 2020.

[63] USDOT. Connected Vehicle Pilot Deployment Program. https://tinyurl.com/y29u9czy, 2019.

[64] USDOT. Intelligent Transportation Systems - Connected Vehicle Basics. https://tinyurl.com/yxjj98vr, 2019.

[65] USDOT. Intelligent Transportation Systems - Connected Vehicle Basics - DSRC. https://tinyurl.com/y5spr5cb, 2019.

[66] USDOT. Intelligent Transportation Systems - Connected Vehicle Pilot Deployment Program. https://tinyurl.com/yy5u7am6, 2019.

[67] USDOT. ITS Standards Program | Standards Group. https://tinyurl.com/yyzb8n4g, 2019.

[68] Veins. Vehicles in network simulation. https://veins.car2x.org/.

[69] VENTOS. Vehicular network open simulator. http://maniam.github.io/VENTOS/, 2019.

[70] M. Wagner and B. McMillin. Cyber-physical transactions: A method for securing vanets with blockchains. In *IEEE PRDC*, 2018.

[71] L. Walkin. ASN.1 Compiler. http://lionet.info/asn1c/, 2019.

[72] Z. Wang, G. Wu, and M. J. Barth. A review on cooperative adaptive cruise control (CACC) systems: Architectures, controls, and applications. In *Proc. ITSC*, 2018.

[73] W. Whyte, J. Petit, V. Kumar, J. Moring, and R. Roy. Threat and countermeasures analysis for WAVE service advertisement. In *Proc. IEEE ITSC*, 2015.

[74] W. Wong, S. Huang, Y. Feng, Q. A. Chen, Z. M. Mao, and H. X. Liu. Trajectory-Based Hierarchical Defense Model to Detect Cyber-Attacks on Transportation Infrastructure. In *Transportation Research Board 2018 Annual Meeting (TRB)*, 2019.

[75] Y. Yu, P. Manolios, and L. Lamport. Model checking TLA$^+$ specifications. In *Proc. CHARME*, 1999.

[76] L. Zhou and Z. J. Haas. Securing ad hoc networks. *IEEE network*, 1999.

A Attack Summary

N2 *Request Mute Attack*: This attack injects a malicious learning response with the same `HashedId8` value of `ca1`. Thus, `V2` chooses to remove the matching entry with the `HashedId8` value of `ca1`. `V2` fails in sending a learning request because `V2` wrongly thinks she has learned the unknown certificate but not.

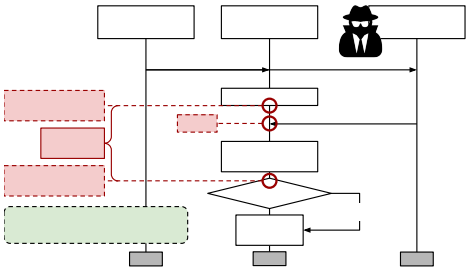

Figure 11: *N2*: the attacker can stop V2 from sending learning requests to V1 by sending a malicious learning requests.

Assumptions. Similar to *N1*, we assume that `V1` does not mandate the verification for incoming learning responses. Also, we assume that the attacker has enough computing power to efficiently construct a learning response that can cause partial hash collision (e.g., low-order 8 bytes collision).

Attack steps. As shown in Figure 11, `V2` initializes P2PCD after receiving a trigger SPDU from `V1`. `V2` stores the `HashedId8` value of the unknown certificate `ca1` in a queue. Meanwhile, since the attacker can observe the trigger SPDU, she constructs a malicious learning response, in which the `HashedId8` value of the first certificate in the payload matches with the unknown certificate `ca1`. As defined in P2PCD, after receiving a learning response, `V2` extracts all certificates in the learning response and stores them via `AddCertificate`. At this time, `V2` wrongly thinks that it has successfully learned the unknown certificate but actually not. Thus, `V2` removes the entry of the unknown certificate `h8(ca1)` in the queue, where `h8` is a function to get the low-order eight-byte hash of the input. As the queue becomes empty, `V2` decides not to attach the learning request in the next outgoing SPDU. Consequently, `V2` is unable to learn the correct unknown certificate.

Discussion. Similar to *N1*, *N2* is also caused by the use of truncated hash, and the attacker does not need to possess a legitimate certificate. In IEEE 1609.2, the issuer field in a certificate is a `HashedId8` value. Therefore, on receiving the trigger SPDU, the vehicle can only store the truncated hash value in the queue. This opens a door for the partial hash collision attack. Although `HashedId8` is larger than `HashedId3` and makes the attacker harder to find a hash collision, a resourceful attacker (e.g., nation-states, terrorists) can always have enough computing power to efficiently find the hash collision. The attacker can even prepare these malicious learning

responses in an offline way. On the other hand, due to the optional verfication of the learning response, it is still possible that some poorly implemented CV protocols may not verify the incoming learning response but just store them.

A4 *Split Trigger Attack*

Assumptions. We assume that the leader keeps the configurations (e.g., platoon size, members) hidden from followers [5].

Attack steps. *A4* requires the attacker to be the leader of the victim platoon, which is consist of `V1` and `V2` sequentially. After becoming the leader, the attacker immediately sends a `SPLIT_REQ` to `V1`. At the last step of the split maneuver, the attacker sends a `SPLIT_DONE` to `V1`, which contains necessary platoon configuration data. Notably, the attacker can control the optimal platoon size in `SPLIT_DONE` and sets it to 1. Since `V1`, as a follower, does not store any platoon configurations, it can only trust the attacker. However, the platoon size exceeds the optimal platoon size; `V1` thus initiates the split maneuver. Most importantly, *A4* leads to a chain reaction that `V1` will pass the wrong configuration to the *last* member in the victim platoon (i.e., `V2` in this case). Moreover, `V1` and `V2` will not able to merge into other platoons or accept any incoming merge requests, because there is no available space.

A5, A6 *Merge Disruption Attack*: The attacker initiates a merge maneuver but does not faithfully complete the whole procedure, so the victim platoon leader `V1` is trapped at the busy state and cannot switch back to the idle state. Therefore, `V1` cannot process any incoming messages.

Attack steps. In *A5*, the attacker first sends a `MERGE_REQ` to `V1`. Since there exists available space in the victim platoon, `V1` will accept the request and send a `MERGE_ACCEPT` to the attacker. In the normal case, `V1` will wait for a `MERGE_DONE` from the merge request initiator. However, the attacker chooses not to send a `MERGE_DONE`; thus, `V1` will keep waiting.

In *A6*, the attacker first utilizes *A2* to join the victim platoon. If `V1` initiates a merge maneuver to join a front platoon and receives a `MERGE_ACCEPT`, `V1` will inform all the followers, including the attacker, to change their platoon leader by sending `CHANGE_PL` to them. The attacker can either passively wait for the happening of the merge maneuver or intentionally trigger the merge maneuver of `V1` by conducting *the platoon takeover attack* (*A1*). As a malicious follower of `V1`, after receiving a `CHANGE_PL` from `V1`, the attacker chooses not to reply with an `ACK`. According to the merge FSM in [5], `V1` will keep sending `CHANGE_PL` to the attacker if `V1` does not receive the corresponding `ACK`.

A8-9 *Split Disruption Attack*: *A8* and *A9* have the same goal and consequence as *A5* and *A6*, but have different attack targets. They focus on vulnerabilities of the split maneuver.

Attack steps. In *A8* and *A9*, the attacker first joins the platoon, which is consist of `V1` (leader) and `V2` sequentially, by launching *A2* and acts as a malicious follower. In *A8*, `V1` sends a `SPLIT_REQ` to the attacker. After accepting the request, the attacker does not respond to the following `CHANGE_PL` sent by `V1`. Therefore, `V1` will not be able to switch back to the idle state. Differently, in *A9*, `V1` sends a `SPLIT_REQ` to `V2`, the splitting vehicle. After `V2` accepting the split request and acknowledging `CHANGE_PL`, `V1` needs to inform the follower behind the attacker to change the platoon leader. The attacker can remain silent, keeping both `V1` and `V2` at the busy state.

A10 *Follower Block Attack*: This attack is the immediate consequence of *A1* and is more powerful than *A5-9*, because this attack can block all vehicles in the victim platoon rather than one or two of them. All members in the victim platoon will be unable to respond any incoming platoon messages.

Attack steps. The attacker first takes over the victim platoon. Then, she sends `SPLIT_REQ` to all her followers (i.e., `V1` and `V2`). `V1` and `V2` accept the split request and reply with `SPLIT_ACCEPT`. Following the protocol, the attacker sends `CHANGE_PL` to `V1` and `V2`. After that, the attacker can drive away or keep silence; all followers thus will never receive `SPLIT_DONE` from the attacker and keep sending `ACK`.

A11 *Gap Attack*: The basic idea of this idea is to prevent the vehicle from "creating" enough space in the front of the splitting vehicle during the leader/follower leave maneuver.

Attack steps. The attacker is the last follower in the victim platoon and initiates a follower leave maneuver. `V1` approves the leave request sent by the attacker. Then, the attacker faithfully respond to `SPLIT_REQ` and `CHANGE_PL` from `V1`. To make the attacker a free agent, `V1` sends a `SPLIT_DONE` to the attacker. Before the completion of the leave maneuver, `V1` has to guarantee that there exists enough space at the front of the attacker to perform lane change. If the attacker does not send a `GAP_CREATED`, `V1` will keep busy as it wrongly thinks the leave maneuver is still on-going.

A12, A13 *Leave Disruption Attack*: *A12* and *A13* exploit timers in the leader leave maneuver and the follower leave maneuver respectively.

Attack steps. In *A12*, when the leader wants to leave the platoon, its followers have to elect a new leader. The elected leader then sends a `ELECTED_LEADER` to the old leader who then hands over the leadership to the elected leader, by initiating the leader leave maneuver and safely leave the platoon. However, if the attacker is one of the followers (*A2*) and becomes the elected leader, she can choose not to respond. As well, *A10* can be used to mislead all followers to a busy state in advance, so no followers can send `ELECTED_LEADER` to the leader, blocking the leader leave maneuver.

In *A13*, a follower wants to leave the platoon and sends a `LEAVE_REQ` to the leader; if no response is received from the leader, the follower is unable to finish the follower leave maneuver. The attacker can place herself at the position of the leader through *A1*, and keep silent. On the other hand, the attacker can utilize *A5-9* to prevent the benign leader from communicating with other followers. Thus, the victim follower cannot finish the follower leave maneuver.

A14 *Dissolve Disruption Attack*: To make a follower unavailable, the attacker can either use *A10* to block all followers or join the victim platoon as a silent follower through *A2*.